

**DETC2003/DAC-48814**

**APPROXIMATE MOTION SYNTHESIS OF OPEN AND CLOSED CHAINS VIA  
PARAMETRIC CONSTRAINT MANIFOLD FITTING: *PRELIMINARY RESULTS***

**Pierre M. Larochelle**

Robotics & Spatial Systems Laboratory  
Department of Mechanical and Aerospace Engineering  
Florida Institute of Technology  
Melbourne, Florida 32901  
Email: pierrel@fit.edu

**ABSTRACT**

*In this paper we present a novel dyad dimensional synthesis technique for approximate motion synthesis. The methodology utilizes an analytic representation of the dyad's constraint manifold that is parameterized by its dimensional synthesis variables. Nonlinear optimization techniques are then employed to minimize the distance from the dyad's constraint manifold to a finite number of desired locations of the workpiece. The result is an approximate motion dimensional synthesis technique that is applicable to planar, spherical, and spatial dyads. Here, we specifically address the planar RR, spherical RR and spatial CC dyads since these are often found in the kinematic structure of robotic systems and mechanisms. These dyads may be combined serially to form a complex open chain (e.g. a robot) or when connected back to the fixed link they may be joined so as to form one or more closed chains (e.g. a linkage, a parallel mechanism, or a platform). Finally, we present some initial numerical design case studies that demonstrate the utility of the synthesis technique.*

**INTRODUCTION**

The constraint manifold of a dyad represents the geometric constraint imposed on the motion of the moving body or workpiece. This geometric constraint on the moving body is a result of the geometric and kinematic structure of the dyad; e.g. its length and the location of its fixed and moving axes (i.e. lines). The constraint manifold is an analytical representation of the workspace

of the dyad that is parameterized by the dyad's dimensional synthesis variables. Here we derive the constraint manifold of spatial CC dyads in the image space of spatial displacements and utilize this constraint manifold to perform dyadic dimensional synthesis for approximate rigid body guidance. Similarly, we derive the constraint manifolds of spherical RR and planar RR dyads in their respected image spaces and utilize their constraint manifolds to perform dyadic dimensional synthesis for approximate motion synthesis.

The derivation of the constraint manifold in the image space involves writing the kinematic constraint equations of the dyad using the components of a dual quaternion. We view these equations as constraint manifolds in the image space of spatial displacements, see [1], [2], and [3]. The result is an analytical representation of the workspace of the dyad that is parameterized by its joint variables. The synthesis goal is to vary the design variables such that all of the prescribed locations are either: (1) in the workspace, or, (2) the workspace comes as close as possible to all of the desired locations. Recall that in general five is the largest number of locations for which an exact solution is possible for the dyads being discussed here, see [4]. Previous works discussing constraint manifold fitting for an arbitrary number of locations include [5], [6], [7], and [2]. All of these works employ *implicit* representations of the dyad constraint manifolds. The constraint manifolds, that are known to be highly nonlinear [8], are then approximated by tangent hyperplanes by using a standard Taylor series linearization strategy. The distance from

the approximating tangent plane to the desired location is then used to formulate an objective function to be minimized. These efforts met with limited success since the constraint manifolds are highly nonlinear and the approximating tangent planes yield poor measures of the distance from the constraint manifold to the desired locations, [9] and [2]. For example, when solving for a spherical four-bar mechanism for 10 desired locations [6] utilized 120 starting cases of which 38 converged to the solution. In [9] a methodology to avoid the difficult nonlinear optimization by using computer graphics to visually present the constraint manifold to the designer was reported. The designer manually manipulated the synthesis variables until the *parameterized* constraint manifold was acceptably near the desired locations. This technique proved to be effective but was tedious to use and results depended heavily upon the designers experience and knowledge. In [10] preliminary work that addressed the synthesis of planar *RR* dyads via parameterized constraint manifold fitting was reported. Here we build upon that work and utilize parameterized constraint manifolds and employ nonlinear optimization to yield a general numerical dimensional synthesis technique for approximate motion synthesis.

We proceed by reviewing the image space of spatial displacements and deriving the parameterized form of the constraint manifold of the spatial *CC* dyad. This is followed by the special cases of spherical and planar displacements and the derivations of the spherical *RR* and planar *RR* dyads, respectively. We then present the general approximate motion synthesis procedure and two initial numerical examples. Future work will further explore the efficiency and robustness of the proposed methodology.

## IMAGE SPACE OF SPATIAL DISPLACEMENTS

First, we review the use of dual quaternions for describing spatial displacements. The general spatial point transformation equation may be written as,

$$\mathbf{X} = [A]\mathbf{x} + \mathbf{d} \quad (1)$$

where  $[A]$  is a  $3 \times 3$  orthonormal rotation matrix representing the orientation of a moving frame  $M$  relative to fixed frame  $F$ , and  $\mathbf{d} = (d_x, d_y, d_z)^T$  is the translation vector from the origin of the frame  $F$  to the origin of frame  $M$ . Associated with the matrix of rotation  $[A]$  is an axis of rotation  $\mathbf{s} = [s_x \ s_y \ s_z]^T$  and a rotation angle  $\theta$ .

Using the translation vector  $\mathbf{d}$ , the rotation axis  $\mathbf{s}$ , and the rotation angle  $\theta$ , we can represent the spatial displacement by the eight dimensional vector  $\mathbf{q}$ , see [3] and [8],

$$\begin{aligned} q_1 &= s_x \sin \frac{\theta}{2} \\ q_2 &= s_y \sin \frac{\theta}{2} \end{aligned} \quad (2)$$

$$\begin{aligned} q_3 &= s_z \sin \frac{\theta}{2} \\ q_4 &= \cos \frac{\theta}{2} \\ q_5 &= \frac{(-d_z q_2 + d_y q_3 + d_x q_4)}{2} \\ q_6 &= \frac{(d_z q_1 - d_x q_3 + d_y q_4)}{2} \\ q_7 &= \frac{(-d_y q_1 + d_x q_2 + d_z q_4)}{2} \\ q_8 &= \frac{(-d_x q_1 - d_y q_2 - d_z q_3)}{2} \end{aligned}$$

We refer to  $\mathbf{q}$  as a dual quaternion. Note that the eight components of  $\mathbf{q}$  satisfy,

$$q_1^2 + q_2^2 + q_3^2 + q_4^2 - 1 = 0$$

and,

$$q_1 q_5 + q_2 q_6 + q_3 q_7 + q_4 q_8 = 0.$$

Because the eight components of  $\mathbf{q}$  satisfy two algebraic constraint equations they form a six dimensional algebraic manifold that we denote as *the image space of spatial displacements*.

## Dual Quaternion Product

Given two dual quaternions  $\mathbf{g}$  and  $\mathbf{h}$  their product yields a dual quaternion that represents the spatial displacement obtained by the successive application of the two given displacements. We may write the product of two dual quaternions in the following matrix form,

$$\mathbf{gh} = G^+ \mathbf{h} = \begin{bmatrix} [g^+] & [0] \\ [g^{0+}] & [g^+] \end{bmatrix} \mathbf{h} \quad (3)$$

where,

$$[g^+] = \begin{bmatrix} g_4 & -g_3 & g_2 & g_1 \\ g_3 & g_4 & -g_1 & g_2 \\ -g_2 & g_1 & g_4 & g_3 \\ -g_1 & -g_2 & -g_3 & g_4 \end{bmatrix}$$

and,

$$[g^{0+}] = \begin{bmatrix} g_8 & -g_7 & g_6 & g_5 \\ g_7 & g_8 & -g_5 & g_6 \\ -g_6 & g_5 & g_8 & g_7 \\ -g_5 & -g_6 & -g_7 & g_8 \end{bmatrix}.$$

Alternatively, we may also write the product of two dual quaternions as,

$$\mathbf{gh} = H^- \mathbf{g} = \begin{bmatrix} [h^-] & [0] \\ [h^{0-}] & [h^-] \end{bmatrix} \mathbf{g} \quad (4)$$

where,

$$[h^-] = \begin{bmatrix} h_4 & h_3 & -h_2 & h_1 \\ -h_3 & h_4 & h_1 & h_2 \\ h_2 & -h_1 & h_4 & h_3 \\ -h_1 & -h_2 & -h_3 & h_4 \end{bmatrix}$$

and,

$$[h^{0-}] = \begin{bmatrix} h_8 & h_7 & -h_6 & h_5 \\ -h_7 & h_8 & h_5 & h_6 \\ h_6 & -h_5 & h_8 & h_7 \\ -h_5 & -h_6 & -h_7 & h_8 \end{bmatrix}$$

### SPATIAL CC CONSTRAINT MANIFOLD

Next, we derive the parametric form of the constraint manifold of the spatial CC dyad. The constraint manifold is derived by expressing analytically the geometric structure that the joints of the dyad impose on the moving body, see [2], [3], [7], and [4]. Using the image space representation of spatial displacements and the geometric constraint equations of the dyad we arrive at a constraint equation in the image space that is parameterized by the dimensional synthesis variables of the dyad.

A spatial 4C mechanism is shown in Fig. (1). A spatial 4C mechanism may be viewed as a combination of two CC dyads. For the moment let us concern ourselves with only one of the dyads which we shall refer to as the *driving dyad*. The driving CC dyad has four independent joint variables,  $\theta$ ,  $d_1$ ,  $\phi$  and  $c_1$  and a link length of  $(\alpha, a)$ . The dimensional synthesis variables of this dyad are  $\mathbf{f}$ ,  $\mathbf{m}$ , and  $(\alpha, a)$  where  $\mathbf{f}$  and  $\mathbf{m}$  are the dual quaternions representing the displacements from the fixed frame to the fixed link frame and from the coupler link frame to the moving frame respectively. We obtain the structure equation in the image space of spatial displacements by using dual quaternions to represent the displacement  $\mathbf{D}$  from  $F$  to  $M$ ,

$$\mathbf{D} = \mathbf{fz}(\theta, d_1)\mathbf{x}(\alpha, a)\mathbf{z}(\phi, c_1)\mathbf{m} \quad (5)$$

where  $\mathbf{x}(\cdot, \cdot)$ ,  $\mathbf{y}(\cdot, \cdot)$ , and  $\mathbf{z}(\cdot, \cdot)$  are dual quaternion representations of spatial displacements either along or about the X, Y, or Z axes respectively. To take full advantage of the image space representation we now rewrite  $\mathbf{D}$  as,

$$\mathbf{D} = \mathbf{gd}'\mathbf{h} \quad (6)$$

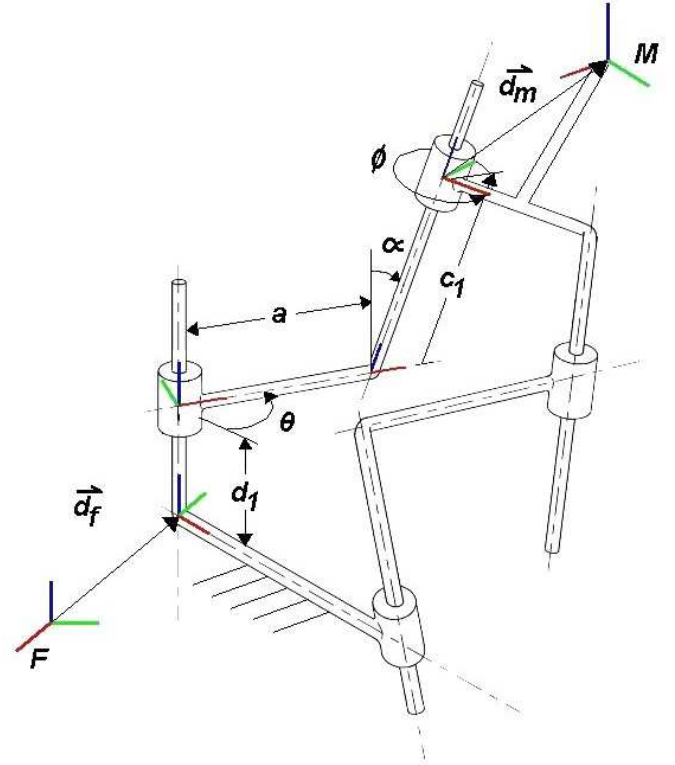


Figure 1. A SPATIAL 4C CLOSED CHAIN

where:  $\mathbf{g} = \mathbf{f}$ ,  $\mathbf{h} = \mathbf{m}$ , and  $\mathbf{d}' = \mathbf{z}(\theta, d_1)\mathbf{x}(\alpha, a)\mathbf{z}(\phi, c_1)$  is the displacement along the dyad. Finally, using Eqns. (3) we express Eqn. (6) as,

$$\mathbf{D}(\theta, d_1, \phi, c_1, \mathbf{r}) = \mathbf{cd}' = G^+ H^- \mathbf{d}'(\alpha, a, \theta, d_1, \phi, c_1) \quad (7)$$

where  $\mathbf{r} = [\mathbf{f}^T \mathbf{m}^T \alpha a]^T$  is the vector of dimensional synthesis variables. In Eqn. (7) we have a hypersurface in the image space of spatial displacements that is parameterized by the design variables of the dyad. This surface is the constraint manifold of the spatial CC dyad parameterized by its four joint variables  $\theta$ ,  $d_1$ ,  $\phi$ , and  $c_1$ . Moreover, it is important to note the arrangement of the design variables in Eqn. (7). All of the joint variables of the dyad have been isolated into the far right-hand-side of Eqn. (7). This arrangement of the design variables will be exploited later by the approximate motion synthesis technique. We now proceed to examine the two special cases of spatial motion; spherical and planar displacements.

### IMAGE SPACE OF SPHERICAL DISPLACEMENTS

First, we review the use of quaternions for describing spherical rigid-body displacements. A general spherical displacement may be described by an axis of rotation  $\mathbf{s} = [s_x \ s_y \ s_z]^T$  and a ro-

tation angle  $\theta$  about said axis. Using  $\mathbf{s}$  and  $\theta$  we can represent a spherical displacement by the four nonzero components of a dual quaternion  $\mathbf{q}$ ,

$$\begin{aligned} q_1 &= s_x \sin \frac{\theta}{2} \\ q_2 &= s_y \sin \frac{\theta}{2} \\ q_3 &= s_z \sin \frac{\theta}{2} \\ q_4 &= \cos \frac{\theta}{2} \end{aligned}$$

We refer to  $\mathbf{q}$  as a quaternion. Note that the four components of  $\mathbf{q}$  satisfy  $q_1^2 + q_2^2 + q_3^2 + q_4^2 - 1 = 0$  and therefore they form a three dimensional algebraic manifold that we denote as *the image space of spherical displacements*.

### 0.1 Quaternion Product

Given two quaternions  $\mathbf{g}$  and  $\mathbf{h}$  their product yields a quaternion that represents the composite spherical displacement. We may write the product of two quaternions in the following matrix form,

$$\mathbf{gh} = G^+ \mathbf{h} = H^- \mathbf{g} \quad (8)$$

where,

$$G^+ = \begin{bmatrix} g_4 & -g_3 & g_2 & g_1 \\ g_3 & g_4 & -g_1 & g_2 \\ -g_2 & g_1 & g_4 & g_3 \\ -g_1 & -g_2 & -g_3 & g_4 \end{bmatrix}$$

and,

$$H^- = \begin{bmatrix} h_4 & h_3 & -h_2 & h_1 \\ -h_3 & h_4 & h_1 & h_2 \\ h_2 & -h_1 & h_4 & h_3 \\ -h_1 & -h_2 & -h_3 & h_4 \end{bmatrix}.$$

### SPHERICAL $RR$ CONSTRAINT MANIFOLD

In this section we derive the parametric form of the constraint manifold of the spherical  $RR$  dyad. We proceed in a similar manner to the spatial  $CC$  dyad. The constraint manifold is derived by expressing analytically the geometric structure that the joints of the dyad impose on the moving body. Using the image space representation of spherical displacements and the geometric constraint equations of the dyad we arrive at constraint

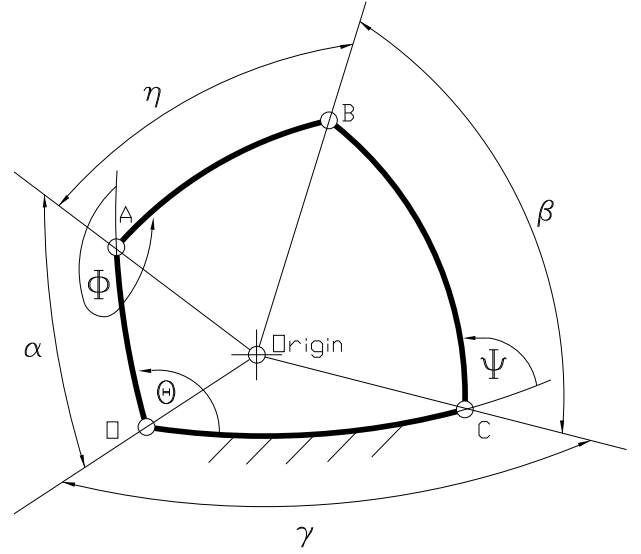


Figure 2. A SPHERICAL 4R CLOSED CHAIN

equations in the image space that are parameterized by the dimensional synthesis variables of the dyad.

A spherical 4R mechanism consisting of two  $RR$  dyads, one of length  $\alpha$ , is shown in Fig. (2). Note that for legibility the fixed and moving frames are not shown in the figure (the fixed frame, moving frame, and all of the link frames have origins coincident at the center of the sphere). The dimensional synthesis variables of this dyad are  $\mathbf{f}$ ,  $\mathbf{m}$ , and  $\alpha$  where  $\mathbf{f}$  and  $\mathbf{m}$  are the quaternions representing the displacements from the fixed frame to the fixed link frame and from the coupler link frame to the moving frame respectively. We obtain the structure equation in the image space of spherical displacements by using quaternions to represent the displacement  $\mathbf{D}$  from F to M,

$$\mathbf{D} = \mathbf{fz}(\theta)\mathbf{x}(\alpha)\mathbf{z}(\phi)\mathbf{m} \quad (9)$$

where  $\mathbf{x}(\cdot)$ ,  $\mathbf{y}(\cdot)$ , and  $\mathbf{z}(\cdot)$  are quaternion representations of displacements about the X, Y, or Z axes respectively. To take full advantage of the image space representation we now rewrite  $\mathbf{D}$  as,

$$\mathbf{D} = \mathbf{gd}'\mathbf{h} \quad (10)$$

where:  $\mathbf{g} = \mathbf{f}$ ,  $\mathbf{h} = \mathbf{m}$ , and  $\mathbf{d}' = \mathbf{z}(\theta)\mathbf{x}(\alpha)\mathbf{z}(\phi)$  is the displacement along the dyad. Finally, using Eqn. (8) we express Eqn. (10) as,

$$\mathbf{D}(\theta, \phi, \mathbf{r}) = \mathbf{cd}' = G^+ H^- \mathbf{d}'(\alpha, \theta, \phi) \quad (11)$$

where  $\mathbf{r} = [\mathbf{f}^T \mathbf{m}^T \alpha]^T$  is the vector of dimensional synthesis variables. In Eqn. (11) we have a surface in the image space of spherical displacements that is parameterized by the design variables

of the dyad. Again, it is important to note the arrangement of the design variables in Eqn. (11). The two joint angles of the dyad have been isolated into the far right hand-side of the expression.

### IMAGE SPACE OF PLANAR DISPLACEMENTS

We now review the use of planar quaternions for describing planar rigid-body displacements. Our approach here is to view planar displacements as a subgroup of  $SE(3)$  and without any loss of generality they are considered as occurring in the  $X - Y$  plane. A general planar displacement may then be described by a  $3 \times 3$  orthonormal rotation matrix  $[A]$  and a translation vector  $\mathbf{d} = [d_x \ d_y \ 0]^T$ . Associated with the matrix of rotation  $[A]$  is an axis of rotation  $\mathbf{s} = [0 \ 0 \ 1]^T$  and a rotation angle  $\theta$ . Using the translation vector  $\mathbf{d}$  and the rotation angle  $\theta$ , we can represent a planar displacement by the four nonzero components of a dual quaternion  $\mathbf{q}$ ,

$$\mathbf{q} = \begin{bmatrix} q_1 \\ q_2 \\ q_3 \\ q_4 \end{bmatrix} = \begin{bmatrix} \frac{d_x}{2} \cos \frac{\theta}{2} + \frac{d_y}{2} \sin \frac{\theta}{2} \\ -\frac{d_x}{2} \sin \frac{\theta}{2} + \frac{d_y}{2} \cos \frac{\theta}{2} \\ \sin \frac{\theta}{2} \\ \cos \frac{\theta}{2} \end{bmatrix}. \quad (12)$$

We refer to  $\mathbf{q}$  as a planar quaternion, see [8]. Note that the four components of  $\mathbf{q}$  satisfy  $q_3^2 + q_4^2 - 1 = 0$  and therefore they form a three dimensional algebraic manifold that we denote as *the image space of planar displacements*.

### Planar Quaternion Product

Given two planar quaternions  $\mathbf{g}$  and  $\mathbf{h}$  their product yields a planar quaternion that represents the composite planar displacement. We may write the product of two planar quaternions in the following matrix form,

$$\mathbf{gh} = G^+ \mathbf{h} = H^- \mathbf{g} \quad (13)$$

where,

$$G^+ = \begin{bmatrix} g_4 & -g_3 & g_2 & g_1 \\ g_3 & g_4 & -g_1 & g_2 \\ 0 & 0 & g_4 & g_3 \\ 0 & 0 & -g_3 & g_4 \end{bmatrix}$$

and,

$$H^- = \begin{bmatrix} h_4 & h_3 & -h_2 & h_1 \\ -h_3 & h_4 & h_1 & h_2 \\ 0 & 0 & h_4 & h_3 \\ 0 & 0 & -h_3 & h_4 \end{bmatrix}.$$

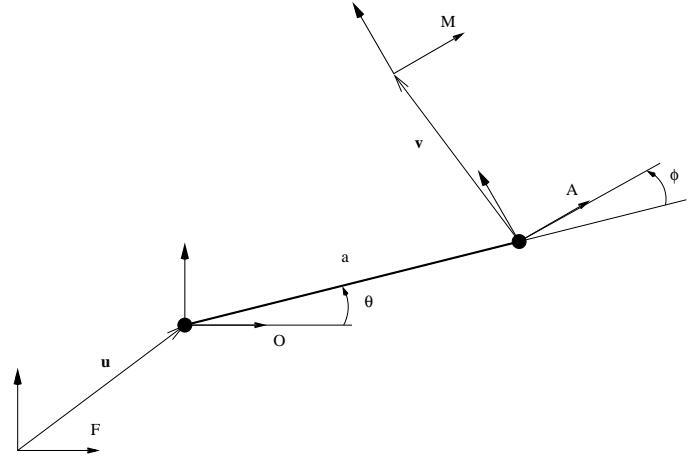


Figure 3. A PLANAR RR DYAD

### PLANAR RR CONSTRAINT MANIFOLD

In this section we derive the parametric form of the constraint manifold of the planar  $RR$  dyad. Again, we proceed as in the cases of the spatial  $CC$  and spherical  $RR$  dyads. Using the image space representation of planar displacements and the geometric constraint equations of the dyad we arrive at constraint equations in the image space that are parameterized by the dimensional synthesis variables of the dyad.

A planar  $RR$  dyad of length  $a$  is shown in Fig. (3). Let the axis of the fixed joint be specified by the vector  $\mathbf{u}$  measured in the fixed reference frame  $F$  and let the origin of the moving frame be specified by  $\mathbf{v}$  measured in the link frame  $A$ . The dimensional synthesis variables of the dyad are  $\mathbf{u}$ ,  $\mathbf{v}$ , and  $a$ . We obtain the structure equation in the image space of planar displacements by using planar quaternions to represent the displacement  $\mathbf{D}$  from  $F$  to  $M$ ,

$$\mathbf{D} = \mathbf{x}(u_x)\mathbf{y}(u_y)\mathbf{z}(\theta)\mathbf{x}(a)\mathbf{z}(\phi)\mathbf{x}(v_x)\mathbf{y}(v_y) \quad (14)$$

where  $\mathbf{x}(\cdot)$ ,  $\mathbf{y}(\cdot)$ , and  $\mathbf{z}(\cdot)$  are planar quaternion representations of displacements either along or about the  $X$ ,  $Y$ , or  $Z$  axes respectively. To take full advantage of the image space representation we now rewrite  $\mathbf{D}$  as,

$$\mathbf{D} = \mathbf{gd}'\mathbf{h} \quad (15)$$

where:  $\mathbf{g} = \mathbf{x}(u_x)\mathbf{y}(u_y)$  is the displacement from  $F$  to  $O$ ,  $\mathbf{h} = \mathbf{x}(v_x)\mathbf{y}(v_y)$  is the displacement from  $A$  to  $M$ , and  $\mathbf{d}' = \mathbf{z}(\theta)\mathbf{x}(a)\mathbf{z}(\phi)$  is the displacement along the dyad from  $O$  to  $A$ .

Performing the quaternion multiplications yields,

$$\mathbf{d}' = \begin{bmatrix} \frac{a}{2} \cos \frac{\theta - \phi}{2} \\ \frac{a}{2} \sin \frac{\theta - \phi}{2} \\ \sin \frac{\theta + \phi}{2} \\ \cos \frac{\theta + \phi}{2} \end{bmatrix} \quad (16)$$

$$\mathbf{g} = \begin{bmatrix} \frac{u_x}{2} \\ \frac{u_y}{2} \\ 0 \\ 1 \end{bmatrix} \quad \text{and} \quad \mathbf{h} = \begin{bmatrix} \frac{v_x}{2} \\ \frac{v_y}{2} \\ 0 \\ 1 \end{bmatrix}. \quad (17)$$

Finally, using Eqn. (13) we express Eqn. (15) as,

$$\mathbf{D}(\theta, \phi, \mathbf{r}) = \mathbf{c}\mathbf{d}' = G^+(\mathbf{u})H^-(\mathbf{v})\mathbf{d}'(a, \theta, \phi) \quad (18)$$

where  $\mathbf{r} = [\mathbf{u}^T \ \mathbf{v}^T \ a]^T$  is the vector of dimensional synthesis variables. In Eqn. (18) we have a surface in the image space of planar displacements that is parameterized by the design variables of the dyad. This surface is the constraint manifold of the planar  $RR$  dyad. Specifically, for a given fixed pivot  $\mathbf{u}$ , a given moving pivot  $\mathbf{v}$ , and a crank length  $a$ , Eqn. (18) yields the constraint manifold of the dyad parameterized by its two joint angles  $\theta$  and  $\phi$ . Again, note that the two joint angles of the dyad have been isolated into the far right hand-side of Eqn. (18).

## APPROXIMATE MOTION SYNTHESIS

In this section we begin by discussing the metric used to measure the distance between the desired image points and the dyad's constraint manifold. This is followed by a numerical synthesis procedure for designing dyads for approximate motion synthesis. It is important to note that the synthesis technique that follows is a general formulation applicable to spatial, spherical, and planar motion synthesis. Hence, the discussion refers to image points in the general sense as they may be spatial, spherical, or planar displacement image points. In order to represent the joint variables in a similarly general manner we utilize the dual angle notation:  $\hat{\theta} = (\theta, d_1)$  and  $\hat{\phi} = (\phi, c_1)$ , see Bottema and Roth (1979). Note that in the cases of spherical and planar syntheses  $d_1 = c_1 = 0$ .

### The Metric

The metric used here to measure the distance  $d$  between an image point  $\mathbf{D}(\hat{\theta}, \hat{\phi}, \mathbf{r})$  on a dyad's constraint manifold and an image point  $\mathbf{q}$  associated with a desired location of the workpiece

is:

$$d(\mathbf{D}(\hat{\theta}, \hat{\phi}, \mathbf{r}), \mathbf{q}) = \sqrt{(\mathbf{D}(\hat{\theta}, \hat{\phi}, \mathbf{r}) - \mathbf{q})^T (\mathbf{D}(\hat{\theta}, \hat{\phi}, \mathbf{r}) - \mathbf{q})}. \quad (19)$$

In order to synthesize dyads that guide the workpiece as near as possible to the desired locations we require an efficient technique for determining the image point  $\mathbf{D}(\hat{\theta}, \hat{\phi}, \mathbf{r})$  that minimizes  $d$ . For a given dyad  $d_{min}$  is determined by performing a direct search of a two dimensional fine discretization of the constraint manifold with respect to  $\hat{\theta}$  and  $\hat{\phi}$ . Note that we exploit the separation of variables in generating the discretization of  $\mathbf{D}(\hat{\theta}, \hat{\phi}, \mathbf{r})$  in Eqs. (7, 11, and 18) since  $G^+$  and  $H^-$  are constant for a given dyad (i.e.  $\mathbf{r}$ ).

It is important to note that  $d$  is a measure of the *distance* from  $\mathbf{D}(\hat{\theta}, \hat{\phi}, \mathbf{r})$  to  $\mathbf{q}$  and that even though this metric is useful for designing dyads it, like all other distance metrics, is variant with respect to choice of coordinate system when used for spatial or planar displacements. For further discussions of displacement metrics see [11], [12], [13], [14], [15], [16], [17], [18], [19], [20], and [21].

## The Optimization Problem

Given a finite set of  $n$  desired locations the task is to determine the dyad that guides the workpiece through, or as near as possible, to these locations. Our approach is to utilize the metric discussed above to determine the distance from the constraint manifold to each of the  $n$  desired locations, sum these distances, and then to employ nonlinear optimization techniques to vary the dimensional synthesis parameters such that the total distance is minimized. The optimization problem then becomes:

MINIMIZE:

$$f(\mathbf{r})$$

where:

$$f(\mathbf{r}) = \sum_{i=1}^n d_{min}(\mathbf{r}, \mathbf{q}_i),$$

We utilize the non-linear optimization package ADS by [22] with the *variable metric method for unconstrained minimization* by [23] and [24].

## The Strategy

The nested optimization strategy is as follows:

1. A candidate design (i.e.  $\mathbf{r}$ ) is selected.

2. A two dimensional fine discretization of the constraint manifold with respect to  $\hat{\theta}$  and  $\hat{\phi}$  is generated. For each desired location the values of the independent joint variables (e.g.  $\hat{\theta}$  and  $\hat{\phi}$ ) are optimized by utilizing the distance metric. The minimum distance to a desired location is  $d_{min}$ . Note that an optimized set of joint variables determines the points on the chain's constraint manifold that are nearest each of the desired locations. This is the inner optimization.
3. The sum of the distances to each of the  $n$  desired locations is determined;  $\sum d_{min}$ . If the distance sum is acceptable then the design is complete. Otherwise, the distance sum and the design vector  $\vec{r}$  are sent to the outer optimization to determine a better candidate design and the above steps are repeated.

Table 1. PLANAR LOCATIONS AND DISTANCES

Pos. #	x	y	$\theta$	Distance
1	0.0	0.0	40.0	$1.10E-4$
2	4.5	4.0	20.0	$5.55E-4$
3	8.5	8.0	0.0	$1.08E-3$
4	13.0	11.5	-30.0	$1.50E-4$
5	13.0	12.5	-35.0	$3.27E-5$
6	9.5	14.0	-35.0	$4.23E-4$
7	5.0	13.5	-30.0	$1.22E-5$
8	1.0	10.5	-15.0	$8.09E-4$
9	-1.0	6.5	0.0	$3.93E-4$
10	-1.5	3.0	20.0	$4.76E-5$

### CASE STUDY: PLANAR OPEN CHAIN

We now present an example of the design of a planar  $RR$  dyad for the ten desired locations that were used by Ravani and Roth to demonstrate their synthesis procedure, see Tbl. (1). The optimal dyad reported by Ravani and Roth was:  $\mathbf{u} = [14.00 \ -0.12]^T$ ,  $\mathbf{v} = [-9.00 \ 1.00]^T$ , and  $a = 8.31$ . This dyad has a distance sum of  $1.03E-2$ . The optimal dyad determined here is:  $\mathbf{u} = [14.98 \ -2.08]^T$ ,  $\mathbf{v} = [-11.22 \ 4.62]^T$ , and  $a = 6.45$ . The distance to each of the desired locations is listed in Tbl. (1) and the distance sum is  $3.62E-3$ . Note that the distance for the synthesis technique presented here is more than 5 times smaller than that for the dyad determined by the constraint manifold linearization technique of Ravani and Roth. Moreover, our implementation of the methodology of Ravani and Roth required more than 50 random initial guesses of the solution to have one converge to the optimal dyad they reported while the technique presented here required only one random initialization to converge to the reported solution.

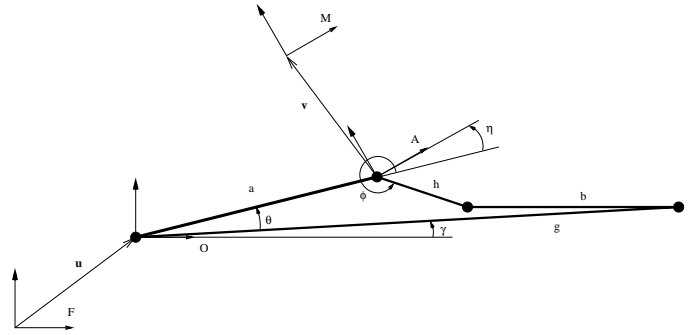


Figure 4. A PLANAR 4R CLOSED CHAIN

where

$$\begin{aligned}
 A &= 2ah - 2gh\cos(\theta) \\
 B &= 2gh\sin(\theta) \\
 C &= a^2 - b^2 + h^2 + g^2 - 2ag\cos(\theta).
 \end{aligned}$$

### CASE STUDY: PLANAR CLOSED CHAIN

A planar  $4R$  closed chain is now created by combining, in parallel, two  $RR$  dyads as shown in Fig. (4). The dimensional synthesis variables of the closed chain are  $\mathbf{u}$ ,  $\mathbf{v}$ ,  $a$ ,  $g$ ,  $h$ ,  $b$ ,  $\gamma$ , and  $\eta$ .

We obtain the constraint manifold of the  $4R$  closed chain from the constraint manifold of the  $RR$  open chain by utilizing the structure equation of the closed chain to obtain  $\phi(\theta)$ :

$$\mathbf{D}(\theta, \mathbf{r}) = \mathbf{c}\mathbf{d}' = G^+(\mathbf{u}, \gamma)H^-(\mathbf{v}, \eta)\mathbf{d}'(a, \theta), \quad (20)$$

where  $\mathbf{r} = [\mathbf{u}^T \ \mathbf{v}^T \ a \ g \ h \ b \ \gamma \ \eta]^T$  is the vector of dimensional synthesis variables and

$$\phi(\theta) = \pm \arccos\left(\frac{-C}{\sqrt{A^2 + B^2}}\right) + \arctan\left(\frac{B}{A}\right)$$

In Eqn. (20) we have a curve in the image space of planar displacements that is parameterized by the joint angle  $\theta$  and this angle has been isolated into the far right hand-side of the expression.

Given a finite set of  $n$  desired locations the task is to determine the closed chain that guides the workpiece through, or as near as possible, to these locations. Our approach is to utilize the metric discussed above to determine the distance from the constraint manifold to each of the  $n$  desired locations, sum these distances, and then to employ nonlinear optimization techniques to vary the dimensional synthesis parameters such that the total distance is minimized. This is the same as the methodology em-

Table 2. PLANAR LOCATIONS AND DISTANCES

Pos. #	x	y	$\theta$	Distance
1	0.0	0.0	40.0	$1.54E-2$
2	4.5	4.0	20.0	$1.77E-2$
3	8.5	8.0	0.0	$3.16E-2$
4	13.0	11.5	-30.0	$1.21E-2$
5	13.0	12.5	-35.0	$3.30E-2$
6	9.5	14.0	-35.0	$2.16E-2$
7	5.0	13.5	-30.0	$4.33E-3$
8	1.0	10.5	-15.0	$5.68E-3$
9	-1.0	6.5	0.0	$1.81E-3$
10	-1.5	3.0	20.0	$9.91E-3$

ployed for the synthesis of open chains. The difference here is that  $\phi$  is now a known function of  $\theta$  whereas in the case of open chains both  $\theta$  and  $\phi$  are independent joint variables. For a given closed chain  $d_{min}$  is determined by performing a direct search of a one dimensional fine discretization of the constraint manifold with respect to  $\theta$ . Note that we again exploit the separation of variables in generating the discretization of  $\mathbf{D}(\theta, \mathbf{r})$ .

For the same ten locations as discussed above we synthesize a planar 4R closed chain. The optimal closed chain is given by:  $\mathbf{u} = [13.72 \ -2.64]^T$ ,  $\mathbf{v} = [-10.41 \ 4.64]^T$ ,  $a = 6.26$ ,  $g = 8.18$ ,  $h = 8.09$ ,  $b = 5.08$ ,  $\gamma = 153.73$ , and  $\eta = 157.16$ . The distance to each of the desired locations is listed in Tbl. (2), the distance sum is  $1.532E-1$ , and the coupler curve of the linkage is shown in Fig. (5). For comparison, the optimal closed chain reported by Ravani and Roth has a distance sum of  $7.295E-1$ .

## CONCLUSIONS

In this paper we have presented a novel dyad dimensional synthesis technique for approximate motion synthesis for a finite number of desired locations of a workpiece. The methodology utilizes an analytic representation of the dyad's constraint manifold that is parameterized by its joint angles. Nonlinear optimization techniques are then employed to minimize the distance from the dyad's constraint manifold to a finite number of desired locations of the workpiece. Algorithms for the synthesis of both open and closed chains are presented. The result is an approximate motion dimensional synthesis technique that is applicable to the design of planar, spherical and spatial dyads. It is important to note that the technique presented utilizes a direct search of the discretization of the constraint manifold and thereby avoids the difficulty of previous techniques that required linearization of

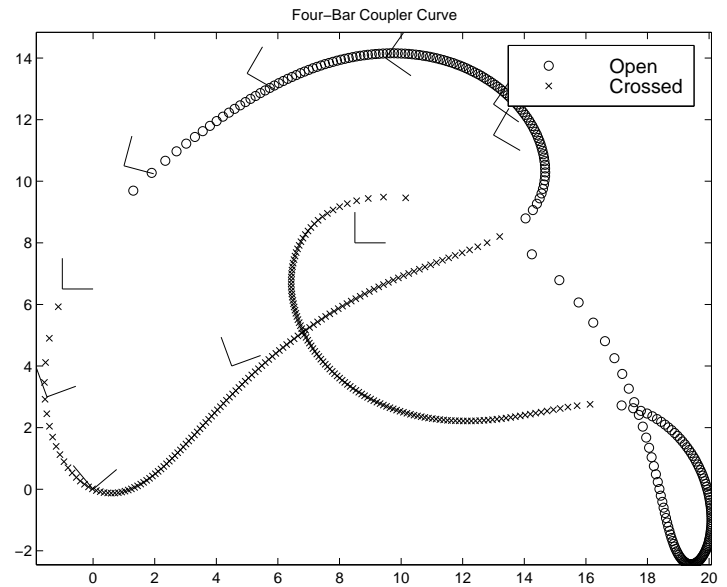


Figure 5. CASE STUDY: SOLUTION COUPLER CURVES

the constraint manifold. Moreover, these dyads are the building blocks of platforms, parallel mechanisms, robots, and linkages and therefore the techniques presented here are directly applicable to their design. Two preliminary planar case studies that serve to illustrate the methodology were presented. Efforts are underway to implement the methodology for the synthesis of spherical and spatial dyads. Continuing work will advance the methodology by incorporating additional design constraints such as order, circuit, mobility, etc. Moreover, we will soon utilize approximate bi-invariant metrics for spatial and planar displacements in the algorithms. Finally, efforts are underway to study the efficiency and robustness of the proposed methodology as it compares to other approximate motion synthesis techniques .

## ACKNOWLEDGEMENTS

The research work reported here was made possible by Grant No. DMI-9816611 from the National Science Foundation.

## REFERENCES

- [1] Bottema, O., and Roth, B., 1979. *Theoretical Kinematics*. North-Holland.
- [2] Larochelle, P., 1994. *Design of Cooperating Robots and Spatial Mechanisms*. PhD Thesis, University of California, Irvine, Irvine, CA.
- [3] Ge, Q., 1990. *The Geometric Representation of Kinematic Constraints in the Clifford Algebra of Projective Space*. PhD Thesis, University of California, Irvine, Irvine, CA.
- [4] Suh, C., and Radcliffe, C., 1978. *Kinematics and Mechanism Design*. John Wiley and Sons.

- [5] Ravani, B., and Roth, B., 1983. "Motion synthesis using kinematic mappings". *ASME Journal of Mechanisms, Transmissions, and Automation in Design*, **105** (1) [September], pp. 460–467.
- [6] Bodduluri, R., and McCarthy, J., 1992. "Finite position synthesis using the image curve of a spherical four bar motion". *ASME Journal of Mechanical Design*, **114** (1) [September], pp. 55–60.
- [7] Bodduluri, R., 1990. *Design and Planned Movement of Multi-Degree of Freedom Spatial Mechanisms*. PhD Thesis, University of California, Irvine, Irvine, CA.
- [8] McCarthy, J., 1990. *An Introduction to Theoretical Kinematics*. MIT Press.
- [9] Larochelle, P., 1996. "Synthesis of planar  $rr$  dyads by constraint manifold projection". In Proceedings of the ASME Design Engineering Technical Conferences, ASME International.
- [10] Larochelle, P., 2000. "Approximate motion synthesis via parametric constraint manifold fitting". In Proceedings of Advances in Robot Kinematics.
- [11] Larochelle, P., and Dees, S., 2002. "Approximate motion synthesis using an svd based distance metric". In Proceedings of Advances in Robot Kinematics.
- [12] Larochelle, P., 1999. "On the geometry of approximate bi-invariant projective displacement metrics". In Proceedings of the World Congress on the Theory of Machines and Mechanisms, vol. 2, IFToMM, pp. 548–553.
- [13] Chirikjian, G., 1998. "Convolution metrics for rigid body motion". In Proceedings of the ASME Design Engineering Technical Conferences, vol. 1, ASME International.
- [14] Larochelle, P., and Tse, D., 1998. "A new method of task specification for spherical mechanism design". In Proceedings of the ASME Design Engineering Technical Conferences, ASME International.
- [15] Larochelle, P., and Tse, D., 2000. "Approximating spatial locations with spherical orientations for spherical mechanism design". *ASME Journal of Mechanical Design*, **122** (4) [December], pp. 457–463.
- [16] Gupta, K., 1997. "Measures of positional error for a rigid body". *ASME Journal of Mechanical Design*, **119** (1) [September], pp. 346–348.
- [17] Bobrow, J., and Park, F., 1995. "On computing exact gradients for rigid body guidance using screw parameters". In Proceedings of the ASME Design Engineering Technical Conferences, vol. 1, ASME International, pp. 839–844.
- [18] Park, F., 1995. "Distance metrics on the rigid-body motions with applications to mechanism design". *ASME Journal of Mechanical Design*, **117** (1) [September].
- [19] Etsel, K., and McCarthy, J., 1996. "A metric for spatial displacements using biquaternions on  $so(4)$ ". In Proceedings of the IEEE Robotics and Automation Conferences, vol. 4, IEEE International, pp. 3185–3190.
- [20] Martinez, J., and Duffy, J., 1995. "On the metrics of rigid body displacements for infinite and finite bodies". *ASME Journal of Mechanical Design*, **117** (1) [September], pp. 41–47.
- [21] Kazerounian, K., and Rastegar, J., 1992. "Object norms: A class of coordinate and metric independent norms for displacements". In Proceedings of the ASME Design Engineering Technical Conferences, ASME International, pp. 271–275.
- [22] Vanderplaats, G., 1984. *ADS - A FORTRAN Program for Automated Design Synthesis*. Naval Post Graduate School.
- [23] Davidon, W., 1959. Variable Metric Method for Minimization. Report ANL-5990, Argonne National Laboratory.
- [24] Fletcher, R., and Powell, M., 1963. "A rapidly-convergent method for minimization". *Computer Journal*, **6** (2) [], pp. 55–60.